Supporting information

Synthesis of Cu(OH)F Microspheres by Atmospheric Dielectric Barrier Discharge Microplasma: A High Performance Non-enzymatic Electrochemical Sensor

Qiang Wang,[a] Li Zhao,[a] Jiaxin Zhou,[a] Zhangmei Hu,[b] Ke Huang,[a] Xue Jiang,*[a] Huimin Yu*[a]

a College of Chemistry and Materials Science, Sichuan Normal University, Chengdu 610068, Sichuan, China

b Analysis and Testing Centre, Southwest Jiaotong University, Chengdu 610030, Sichuan, China.

**E-mail: jiangxue@sicnu.edu.cn (X.J.); yuhuimin208@sicnu.edu.cn (H.Y.)*

Experimental Section

1. Schematic diagram of microplasma experiment device

Schema. 1 presents a simple structure of a dielectric barrier discharge (DBD) reactor, which consists of one large and one small hollow concentric glass cylinder (The large cylinder is open at the top and closed at the bottom, while the small cylinder is closed at the top and open at the bottom. And the reactants and carbon cloth are placed in the gap between the large and small glass cylinders.), a copper rod, and a copper wire. The copper wire is tightly wound on the outside of the large glass tube. The copper rod is inserted into the small cylindrical glass tube. And both the copper wire and the copper rod are connected to the power source. After turning on the power, bright blue plasma was observed in the reactor.

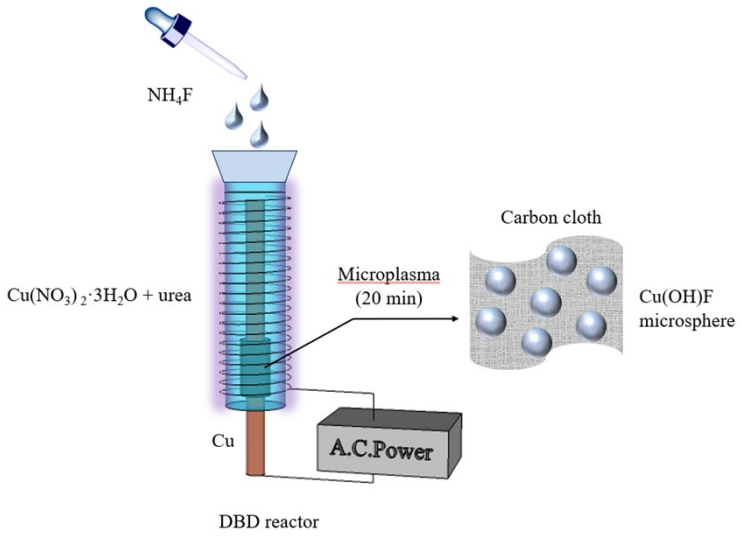

Schema. 1

2. Reagents and materials

Glucose (Glu), NaCl, KH_2PO_4, $K_2HPO_4·3H_2O$, HCHO, ethanol, CH_3CHO, 1-propanol, $NaNO_3$, H_2O_2 and NaOH were purchased from Kelong reagent Co. Ltd. (Chengdu, China). $Cu(NO_3)_2·3H_2O$ was purchased from J&K Chemicals Technology Co. Ltd. (Beijing, China). Urea, ascorbic acid (AA), NH_4F, uric acid (UA), lactose, fructose were purchased from Wokai biotechnology Co. Ltd. (Shanghai, China). Dopamine Hydrochloride was obtained from Macklin biological reagent Co. Ltd. (Shanghai, China). All of above reagents were used directly without further dispose. Carbon cloth (CC) was purchased by Hongshan District, Wuhan Instrument Surgical Instruments business. All solutions were prepared with deionized water.

3. Preparation of Cu(OH)F MS/CC

To remove the surface impurities, CC was treated with nitric acid at 120 °C for 2 hours, and then washed several times with ethanol. Cu(OH)F MS/CC was prepared in-situ by microplasma. Briefly, 1.21 g $Cu(NO_3)_2 \cdot 3H_2O$ and 1.44 g urea were dissolved in 50 mL ultrapure water, and 1.05g NH_4F were dissolved in 50 mL ultrapure water. Cut a small piece of cleaned carbon cloth (1cm × 3cm) to the bottom of the glass tube, and then use a disposable dropper to absorb about 3 ml of the $Cu(NO_3)_2 \cdot 3H_2O$ and urea solution into the DBD reactor. Then, the microplasma voltage was adjusted to 90 V and added NH4F solution into the reactor drop by drop. After 20 min, the Cu(OH)F MS/CC was synthesized. Finally, Cu(OH)F MS/CC was dried at 70 °C for 3 hours to use. Fig.S1 reveals the synthesis voltage and time optimization.

4. Characterization

X-ray diffraction (XRD) measurements were operated on a RigakuD/MAX 2550 diffractometer with Cu Kα radiation (λ = 1.5418 Å). Scanning electron microscope (SEM) data were collected from a Quanta 250 Scanning electron microscope (FEI Instrument Co. USA) at an accelerating voltage of 20 kV. X-ray photoelectron spectroscopy (XPS) spectra were tested by an ESCALABMK II X-ray photoelectron spectrometer by Mg-Kα X-ray as exciting source. High resolution transmission electron microscopy (HRTEM) images were obtained by a JEOL JEM-2100 transmission electron microscope (JEOL Ltd, Tokyo, Japan) at 200 kV.

5. Electrochemical measurements

In this work, electrochemical measurements were operated on a CHI 660E electrochemical workstation of CH Instruments (Shanghai, China). The electrolyte was a 0.1 M sodium hydroxide (NaOH) aqueous solution for the glucose/HCHO and 0.1 M PBS for the H_2O_2 sensor. Standard three-electrode system with platinum wire as the counter electrode, Cu(OH)F MS/CC as the working electrode, and the Hg/HgO and Ag/AgCl electrode as the reference electrode.

6. Discussion section of formaldehyde detection.

Fig. S6a reveals that in the 0.1M NaOH solution and the scan rate is 50 mV s^{-1}, the CV curve 1 is the experimental result of the empty carbon cloth without dropping HCHO. Curve 2 is the CV curve measured under the same other conditions after the dropwise addition of 2 mM HCHO aqueous solution, revealing that the impact of the empty carbon cloth on the detection of HCHO is negligible. Then, Cu(OH)F MS/CC obtained curve 3 with a redox peak without dropping HCHO. On this basis, after dropping 2 mM HCHO, the peak current of the oxidation peak increased (curve 4), indicating that Cu(OH)F MS/CC has an electrocatalytic oxidation effect on HCHO. Fig. S6b shows the obvious anodic oxidation peak on the CV curve when Cu(OH)F MS/CC electrode is used. As the concentration of HCHO increased from 0 mM to 14 mM, the current response of anodization gradually increased.

In order to study the effect of scanning rate on the oxidation of HCHO. Fig. S7a shows that when the scan rate is increased from 20 mV s^{-1} to 200 mV s^{-1}. Thus, the linear relationship between the peak current density and square root of the scan rate in Fig. S7b is obtained. This indicates that the oxidation of HCHO by Cu(OH)F is affected by the diffusion of the tested substance, which is a process of diffusion control.

The test potential optimization is shown in Fig. S8. According to the optimization results, this paper selects 0.55 V as the optimal test potential of HCHO in 0.1 M NaOH. Fig. S6c reveals an i-t curve where the current density increases with increasing HCHO concentration at a test voltage of 0.55 V. The small graph shows the ampere current response when the HCHO concentration range (4 μM-40 μM) changes. It can also be seen that with the increasing amount of HCHO, the current density increases rapidly and the electrode has a fast ampere response, which can reach a stable current density within 5 s. With the increase of formaldehyde concentration, the current density corresponding to the concentration showed a good linear relationship within a certain range and a wider detection range of 4 μM-7.45 mM (4 μM-2.45 mM and 2.45 mM-7.45 mM) was obtained. The linear relationship is shown in Fig. S6d, and a lower detection limit (0.157 μM, S/N = 3) and high sensitivity (3929.0 μA mM^{-1} cm^{-2}) are obtained. The performance comparison with the reported HCHO non-enzymatic electrochemical sensor is shown in Table S2. Fig. S6e shows the experimental results of adding 1 mM HCHO and 0.1 mM interfering substances at a test potential of 0.55 V, respectively. It can be seen that the influence of the current change caused by the interference on the formaldehyde test can be ignored.

Fig. S6f verifies the reliability of our sensor for HCHO detection. The standard addition method was used to determine the HCHO content in tap water and pool water, and the results are shown in Table S4. According to the data in the table, the recovery ratios of 20.0 μM and 25.0 μM formaldehyde in real samples of tap water and pool water are between 98.0 and 101.0%. This shows that the Cu(OH)F MS/CC sensor has high reliability for formaldehyde sensing and can be expected to be applied in practice.

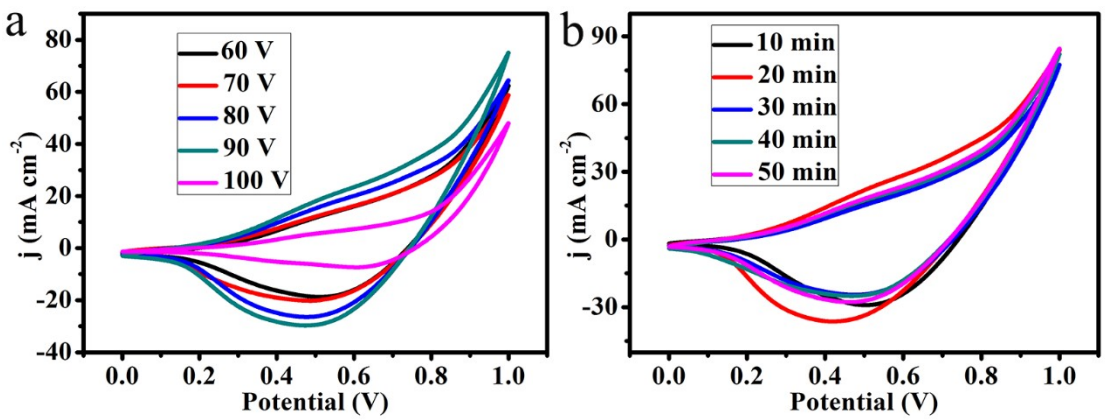

Fig. S1. (a) The CV curves of Cu(OH)F MS/CC with 1 mM glucose in 0.1 M NaOH with the scan rate at 50 mV s^{-1} and the microsphere synthesized under 60, 70, 80, 90 and 100 V conditions at the same synthetic time. (b) The CV curves of Cu(OH)F MS/CC with 1 mM glucose in 0.1 M NaOH with the scan rate at 50 mV s^{-1} and the microsphere synthesized under 10, 20, 30, 40 and 50 min conditions at the same synthetic voltage.

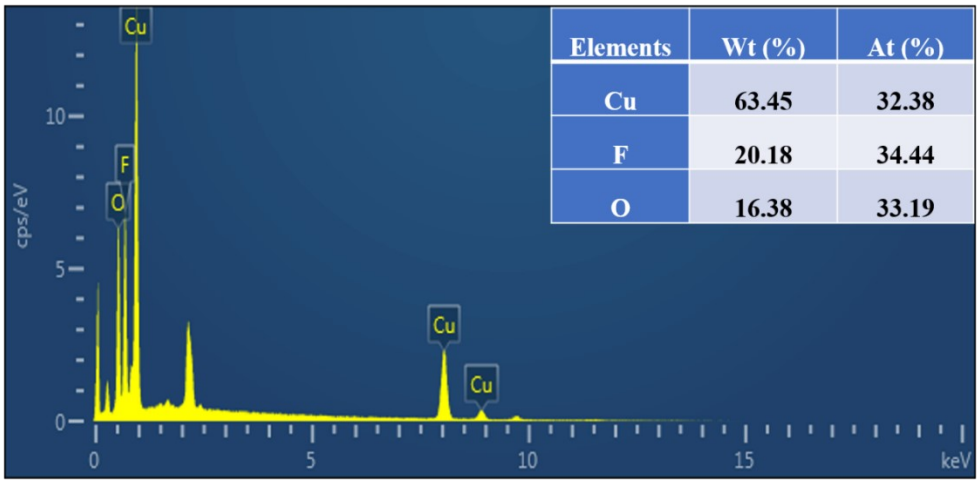

Elements	Wt (%)	At (%)
Cu	63.45	32.38
F	20.18	34.44
O	16.38	33.19

Fig. S2. EDX spectrum of Cu(OH)F; the inset table shows the elemental composition of Cu(OH)F.

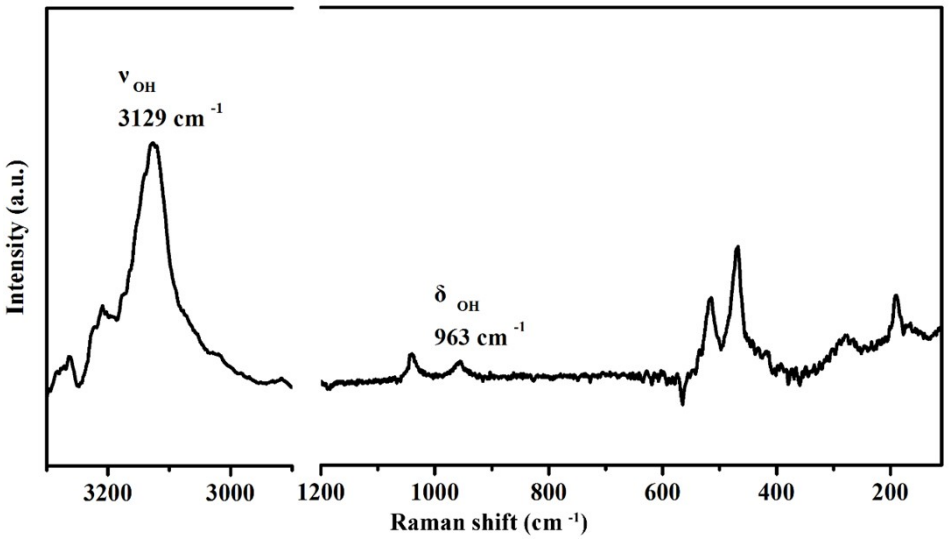

Fig. S3. Raman scattering spectra of Cu(OH)F.

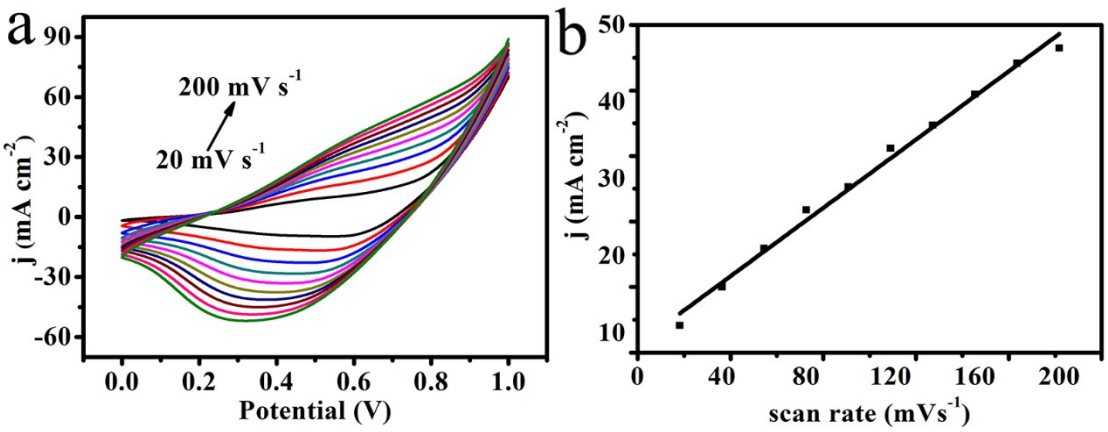

Fig. S4. (a) The CV curves of Cu(OH)F MS/CC in 1 mM glucose of scan rates starting from 20 mV s^{-1} and ending at 200 mV s^{-1}. (b) The corresponding plots of current density vs. the scan rate.

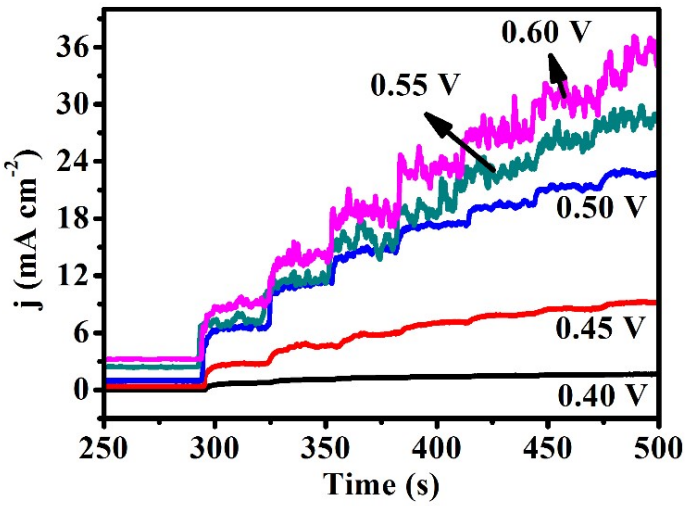

Fig. S5. Amperometric responses of Cu(OH)F MS/CC at different potentials (0.40-0.60 V) with continuous addition of 1 mM glucose in 0.1 M NaOH.

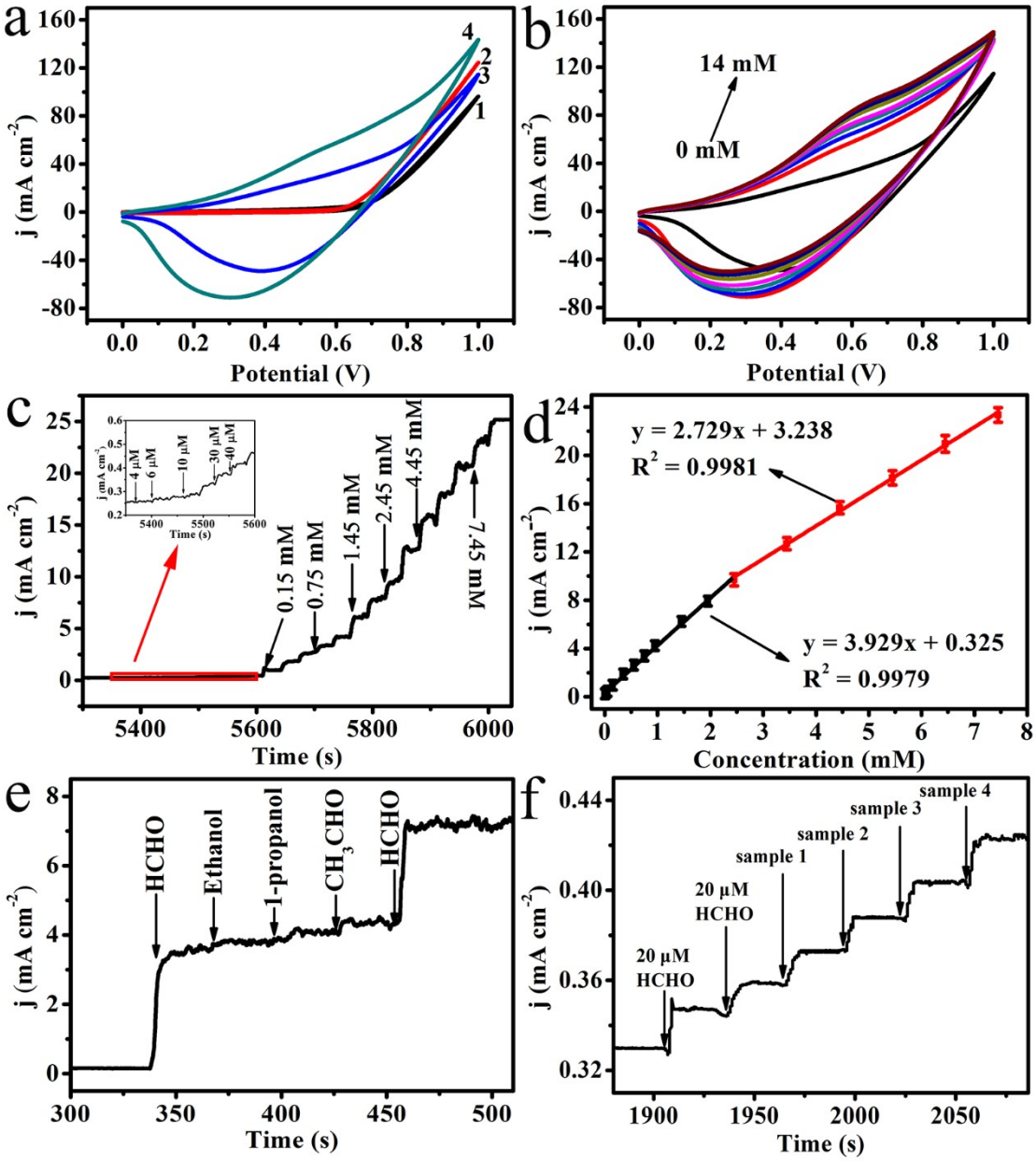

Fig. S6. (a) The CV curves of carbon cloth and Cu(OH)F MS/CC (curve 1, 2 and 3,4) in 0.1 M NaOH without (curve 1 and 3) and with (curve 2 and 4) 2 mM HCHO at 50 mV s^{-1} scan rate.(b) CVs for Cu(OH)F MS/CC in 0.1 M NaOH at the presence of varied HCHO concentrations (0 mM to 14 mM; scan rate: 50 mV s^{-1}). (c) Amperometric response of Cu(OH)F MS/CC with successive addition of HCHO in 0.1 M NaOH (inset: the current response of electrode toward the addition of HCHO from 4 to 40 μM). (d) the corresponding calibration curve of Cu(OH)F MS/CC electrode to successive additions of HCHO at 0.55 V in 0.1 M NaOH. (e) Amperometric response of Cu(OH)F MS/CC electrode towards the addition of HCHO (1 mM) and different interfering compounds (0.1 mM) in 0.1 M NaOH. (f) Amperometric response of the Cu(OH)F MS/CC on addition of 20 μM HCHO and four samples at an applied potential of 0.55 V in 0.1 M NaOH solution.

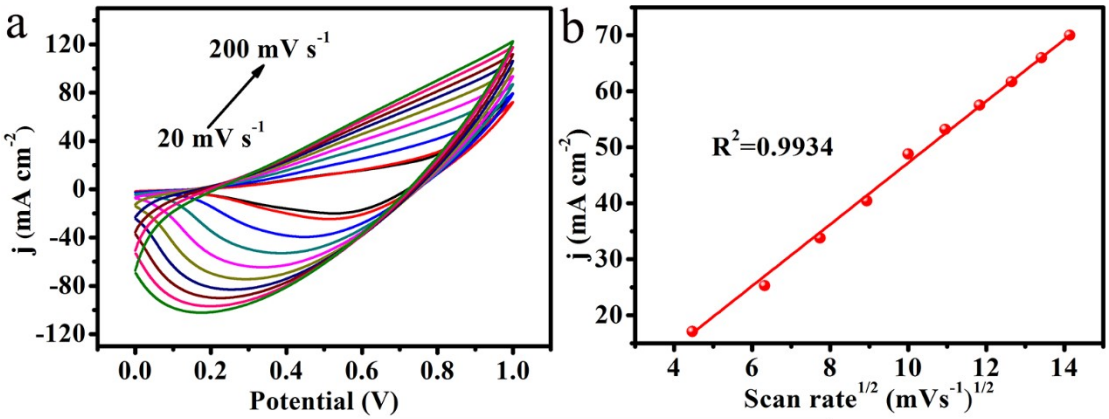

Fig. S7. (a) The CV curves of Cu(OH)F MS/CC in 1 mM HCHO of scan rates starting from 20 mV s^{-1} and ending at 200 mV s^{-1}. (b) The corresponding plots of current density vs. the scan $rate^{1/2}$.

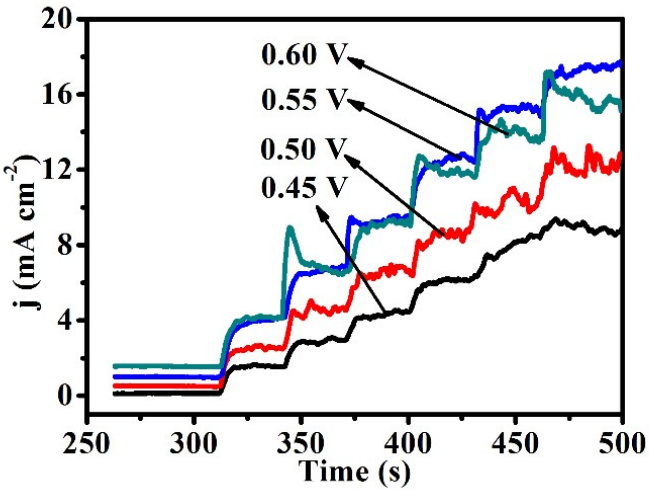

Fig. S8. Amperometric responses of Cu(OH)F MS/CC at different potentials (0.45, 0.50, 0.55, and 0.60 V) with continuous addition of 1 mM HCHO in 0.1 M NaOH.

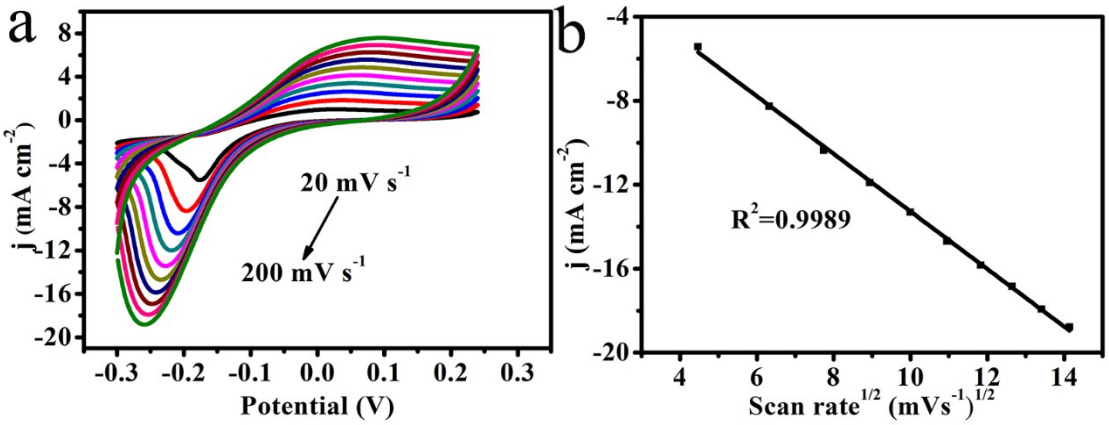

Fig. S9. (b) The CV curves of Cu(OH)F MS/CC in PBS (pH = 7.0) with 1 mM H_2O_2 of scan rates starting from 20 and ending at 200 mV s^{-1}.

(c) The corresponding plots of current density vs. the square root of scan rate.

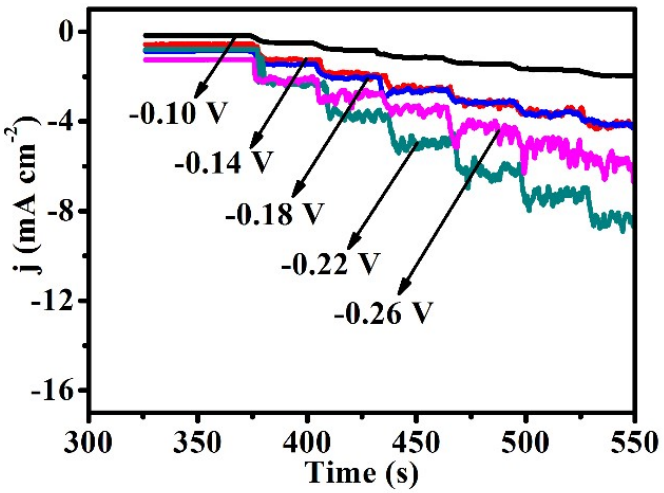

Fig. S10. Amperometric responses of Cu(OH)F MS/CC at different potentials (-0.10, -0.14, -0.18, -0.22 and -0.26 V) with continuous addition of 1 mM H_2O_2 in 0.1 M PBS.

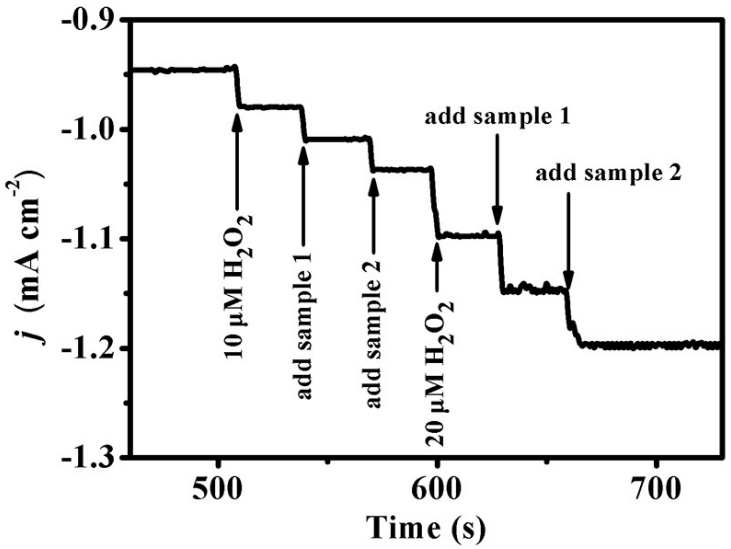

Fig. S11. Amperometric response of the Cu(OH)F MS/CC on addition of H_2O_2 and two serum samples at an applied potential of -0.22 V in PBS solution.

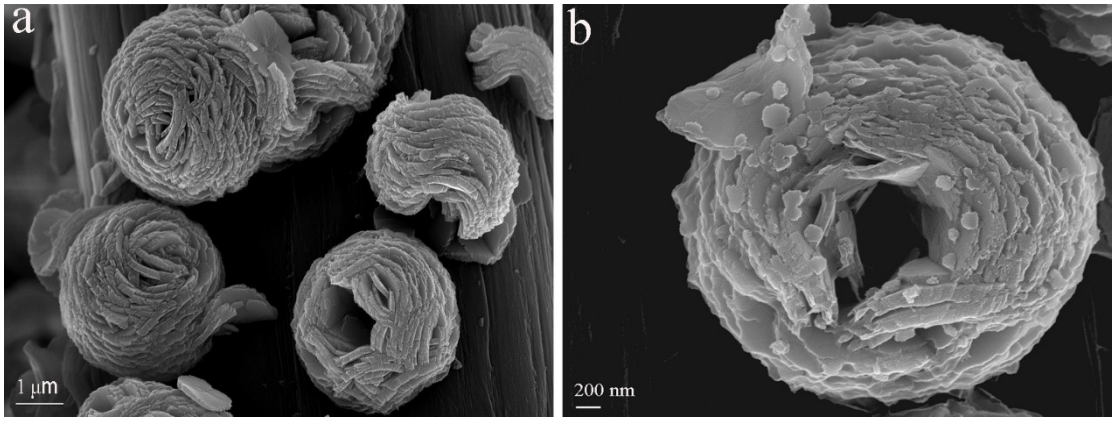

Fig. S12. SEM images for Cu(OH)F MS/CC after electrochemical detection.

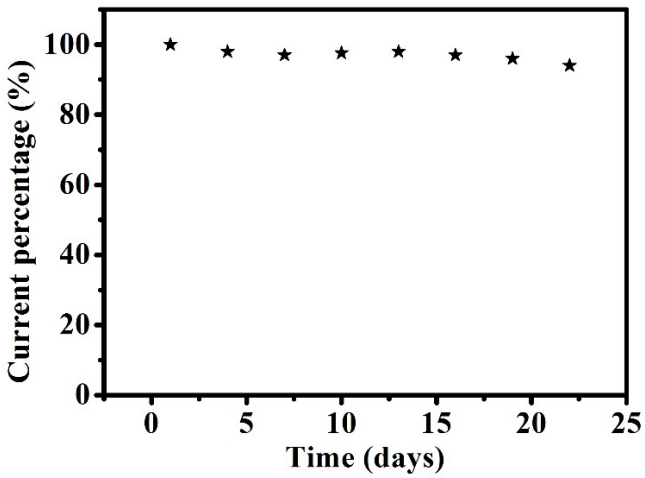

Fig. S13. Normalized sensitivity of Cu(OH)F MS/CC as the working electrode to formaldehyde tested every 3 days within a month.

Table S1. Comparison of the performances of our catalysts toward other reported glucose biosensors

Electrodes	Sensitivity ($\mu A\ mM^{-1}\ cm^{-2}$)	Linear range (m M)	LOD (μM)	References
CuS MF	1007	0.02–5.4	2.0	1
Cu micropillar arrays	2432	0.0005–4.711	0.19	2
CuO nanourchins	2682	0.1–3	1.52	3
Cu nanoparticles/reduced graphene oxide	447.65	Up to 1.2	3.4	4
CuO NWs/ Cu foil	1420.3	Up to 2.05	5.1	5
Ni-Cu/TiO_2NTs	1590	Up to 3.2	5.0	6
CuO NS/CC	4901.96	Up to 1.0	1.0	7
Cu(OH)F MS/CC	4083.0	0.001–7.45	0.408	this work

Table S2. Comparison of the performances of our catalysts toward other reported formaldehyde biosensors

Electrodes	Sensitivity ($\mu A\ mM^{-1}\ cm^{-2}$)	Linear range (m M)	LOD (μM)	References
Ni/P-CPE	–	0.02–11.5	5.8	8
$Ni(OH)_2$/Ni/TNAs	2110	0.065–8.775	33.4	9
CuO/GCE	68.6	0.001–10	0.25	10
Fe@Pt/C	40.18	0.0125–15.4	3.75	11
Pd NW/GCE	1360	0.002–1	0.5	12
Cu(OH)F MS/CC	3929.0	0.004–7.45	0.157	this work

Table S3. Comparison of the performances of our catalysts toward other reported hydrogen peroxide biosensors

Electrodes	Sensitivity ($\mu A\ mM^{-1}\ cm^{-2}$)	Linear range (m M)	LOD (μM)	References
Pt-IL-pGR	942.15	0.01–4.0	0.42	13
Graphene/pectin-CuNPs	391.0	0.001–1.0	0.35	14
Cu_2O/Ag Composite	–	0.05–0.5	4.0	15
Cu_2O/Cube/Graphene Nanosheet	–	0.3–7.8	20.8	16
Cu_2O microspheres/RGO	–	0.005–2.775	10.8	17
Cu(OH)F MS/CC	1136.0	0.003–9.45	1.48	this work

Table S4. Testing of real samples of glucose, formaldehyde and hydrogen peroxide

Glucose	Sample	Measured by glucometer (mM)	Determined by our sensor (mM)	RSD(%) (n=3)
	1	6.1	6.6	1.6
	2	5.3	5.6	1.9
HCHO	Sample	Amount of standard HCHO added (μM)	Amount of HCHO found (μM)	Recovery (%)
	Tap water	20.0	20.2	101.0
		25.0	24.8	99.2
	Pool water	20.0	19.7	98.5
		25.0	24.6	98.4
H_2O_2	Sample	Amount of standard H_2O_2 added (μM)	Amount of H_2O_2 found (μM)	Recovery (%)
	Tap water	20.0	20.13	100.6
		15.0	14.2	94.6

Table S5. Determination of H_2O_2 in human blood serum samples using Cu(OH)F MS/CC electrode.

	Sample	Amount of standard H_2O_2 added (μM)	Amount of H_2O_2 found (μM)	Recovery (%)
H_2O_2	Serum 1	10.0	9.8	98.0
		20.0	19.7	98.5
	Serum 2	10.0	9.7	97.0
		20.0	19.6	98.0

References

1. S. Radhakrishnan, H. Y. Kim and B. S. Kim, *Sens. Actuators, B*, 2016, **233**, 93-99.
2. M. M. Guo, Y. Xia, W. Huang and Z. L. Li, *Electrochim. Acta*, 2015, **151**, 340-346.
3. S. D. Sun, X. Z. Zhang, Y. X. Sun, S. C. Yang, X. P. Song and Z. M. Yang, *ACS Appl. Mater. Interfaces*, 2013, **5**, 4429-4437.
4. Q. Wang, Q. Wang, M. S. Li, S. Szunerits and R. Boukherroub, *RSC Adv.*, 2015, **5**, 15861-15869.
5. Y. C. Li, M. G. Zhao, J. Chen, S. S. Fan, J. J. Liang, L. J. Ding and S. G. Chen, *Sens. Actuators, B*, 2016, **232**, 750-757.
6. X. L. Li, J. Y. Yao, F. L. Liu, H. C. He, M. Zhou, N. Mao, P. Xiao and Y. H. Zhang, *Sens. Actuators, B*, 2013, **181**, 501-508.
7. Y. Zhong, T. L. Shi, Z. Y. Liu, S. Y. Cheng, Y. Y. Huang, X. X. Tao, G. L. Liao and Z. R. Tang, *Sens. Actuators, B*, 2016, **236**, 326-333.
8. S. N. Azizi, S. Ghasemi and F. Amiripoura, *Sens. Actuators, B*, 2016, **227**, 1-10.
9. X. Wen, J. J. Xi, M. Long, L. Tan, J. J. Wang, P. Yan, L. F. Zhong, Y. Liu and A. D. Tang, *J. Electroanal. Chem.*, 2017, **805**, 68-74.
10. Z. H. Jing and X. Q. Lin, *Chinese J. Chem.*, 2010, **28**, 2359-2363.
11. H. Mei, W. Q. Wu, B. B. Yu, H. M. Wu, S. F. Wang and Q. H. Xia, *Sens. Actuators, B*, 2016, **223**, 68-75.
12. Y. Zhang, M. Zhang, Z. Q. Cai, M. Q. Chen and F. L. Cheng, *Electrochim. Acta*, 2012, **68**, 172-177.
13. H. S. Zhang, X. J. Bo and L. P. Guo, *Electrochim. Acta*, 2016, **201**, 117-124.
14. V. Mani, R. Devasenathipathy, S. M. Chen, S. F. Wang, P. Devi and Y. Tai, *Electrochim. Acta*, 2015, **176**, 804-810.
15. W. H. Antink, Y. Choi, K. D. Seong and Y. Piao, *Sens. Actuators, B*, 2018, **255**, 1995-2001.
16. M. M. Liu, R. Liu and W. Chen, *Biosens. Bioelectron.*, 2013, **45**, 206-212.
17. J. W. Ding, W. Sun, G. Wei and Z. Q. Su, *RSC Adv.*, 2015, **5**, 35338-35345.